Light response curve methodology and possible implications in the 2 application of chlorophyll fluorescence to benthic diatoms

Rupert G. Perkins, Jean-Luc Mouget, Sébastien Lefebvre, Johann Lavaud

Light response curve methodology and possible implications in the application of chlorophyll fluorescence to benthic diatoms

Perkins, R.G.[1*], Mouget, J-L.[2], Lefebvre, S.[3] and Lavaud, J.[4]

1. School of Earth, Ocean and Planetary Sciences, Cardiff University, Main Building, Park Place, Cardiff, UK CF10 3YE

2. Laboratoire de Physiologie et Biochimie Végétales, Faculté des Sciences et Techniques, Université du Maine, EA2663, Av. O. Messiaen, 72085 Le Mans Cedex 9, France.

3. Laboratoire de Biologie et Biotechnologies Marines, Esplanade de la Paix, EA 962 Université de Caen, 14032 Caen Cedex, France.

4. Pflanzliche Ökophysiologie, Fachbereich Biologie, Universität Konstanz, Universitätsstraße 10, 78457 Konstanz, Germany.

*Corresponding author: Tel. +44 (0)29 208 74943; Fax: +44 (0)29 208 74326; Email: PerkinsR@cf.ac.uk

Abstract

Chlorophyll *a* fluorescence has been increasingly applied to benthic microalgae, especially diatoms, for measurements of electron transport rate (ETR) and construction of rapid light response curves (RLCs) for the determination of photophysiological parameters (mainly the maximum relative ETR ($rETR_{max}$), the light saturation coefficient (E_k) and the maximum light use coefficient). Various problems with the estimation of ETR from the microphytobenthos have been identified, especially *in situ*. This study further examined the effects of light history of the cells and light dose accumulation during RLCs on the fluorescence measurements of ETR using the benthic diatom *Navicula phyllepta*. RLCs failed to saturate when using incremental increases in irradiance, however curves with decreasing irradiance did saturate. Patterns indicating photoacclimation in response to light histories were observed, with higher $rETR_{max}$ and E_k, and lower α, at high light compared to low light. However these differences could be negated by increasing the RLC irradiance duration from 30 to 60 s. It is suggested that problems arose as a result of rapid fluorescence variations due to ubiquinone, Q_A, oxidation and non-photochemical chlorophyll fluorescence quenching, NPQ, which depended upon the light history of the cells and the RLCs accumulated light dose. Also, RLCs with irradiance duration of 10 s were shown to have an error possibly specific to the fluorimeter programming. It is suggested that RLCs, using a Diving-PAM fluorimeter on benthic diatoms, should be run using decreasing irradiance steps of 30 s duration.

Introduction

Benthic microalgae communities, mainly composed of diatoms, inhabit shallow estuarine intertidal sediments where they are responsible for the major part of the photosynthetic primary production (MacIntyre et al., 1996). The light environment to which the microphytobenthos are exposed is highly variable due to the tidal regime, which expose the cells to a wide range of, and rapid changes between, levels of irradiance, together with a high spatial and temporal frequency of light fluctuations. Therefore, one the main challenges for microphytobenthic algae is to cope with fluctuations in irradiance, largely through avoidance of energy imbalance within the photosynthetic apparatus, and maintainance of an optimal irradiance to maximise photosynthetic productivity (Underwood and Kromkamp, 1999, Perkins et al 2002, Consalvey et al. 2005a). For this purpose, algae have evolved a number of mechanisms referred to as photoacclimation (MacIntyre et al. 2000, Raven and Geider, 2003).

To investigate the photosynthesis of the microphytobenthos, chlorophyll *a* (Chl *a*) fluorescence measurements of electron transport rate (ETR) and related photophysiological parameters are being increasingly applied (Consalvey et al. 2005a). Studies have been used to compare measurements of primary productivity using different methodologies, principally carbon uptake (radio-labeled ^{14}C), electron transport rate (Chl *a* fluorescence) and oxygen evolution (oxygen electrodes) (Flameling & Kromkamp 1998, Hartig et al. 1998, Barranguet and Kromkamp 2000, Perkins et al. 2001, 2002). Others have been confined solely to the use of Chl *a* fluorescence as a proxy for primary productivity by measuring ETR (Kromkamp et al. 1998; Serôdio and Catarino 2000; Serôdio 2003; Serôdio et al. 2005a; Underwood et al. 2005) or as a proxy for algal biomass (Serôdio et al. 1997; Honeywill et al. 2002).

The recent technique of rapid light response curves (RLCs), defined as very short (tens of seconds) light steps of different intensity, has been widely applied for the determination of ETR versus irradiance on different photosynthetic aquatic organisms like macro-and micro-algae, seagrasses and corals (Schreiber et al. 1997, Ralph et al. 1999, Kühl et al. 2001, Glud et al. 2002, Ralph and Gademann 2005). The short duration of each light step is an attempt to minimize the confounding effects of light acclimation encountered with 'steady-state' traditional light curves (Serôdio 2004, Serôdio et al. 2005a). RLCs have been used with success on microphytobenthos assemblages isolated from the field or directly *in situ* (Perkins et al. 2002, Serôdio et al. 2005a). However, the assessment of RLCs on intact biofilms can be disturbed, which may alter the calculation of ETR as a function of light intensity (Perkins et al. 2002). The two major sources of disturbance that have been identified are the attenuation of light in the sediment and the depth-integration of fluorescence emitted from sub-surface layers (Forster and Kromkamp 2004, Serôdio 2004), and the migration of the cells within the biofilm (Kromkamp et al. 1998, Perkins et al. 2002, Serôdio 2004). In addition, rapid as well as endogenous changes in photosynthesis activity, which modulate the Chl *a* fluorescence emission, can potentially affect ETR measurements (Serôdio et al. 2005a). In particular, the red-ox state of Q_A, the primary PSII electron acceptor, and non-photochemical Chl *a* fluorescence quenching (NPQ) have been shown to influence the fluorescence measurements in microphytobnethic diatoms (Consalvey et al. 2004, Serôdio et al. 2005a, 2005b). In this context, technical features of the RLCs, such as the length of each irradiance step, have been shown to be important for the assessment of ETR (Serôdio et al. 2005a).

This study aimed to further improve the use of Chl *a* fluorescence measurements for the construction of RLCs for application to benthic algae. We

especially focused on the ability of the RLCs to relate the photoacclimation status through the assessment of ETR. By using algal cultures of the benthic diatom, *Navicula phyllepta* Kützing, we investigated the effect on the ETR/light relationship of: 1) the light history of the cells, 2) the RLCs light step duration and order (i.e. increasing or decreasing irradiance). The data obtained were compared with RLCs performed on separate replicates of the culture for each light step ('non sequential' light curves, N-SLCs) to assess the potential cumulative effect of rapid photoacclimation of the cells during the light curve itself. The results raise important questions with regard to potential errors in the measurement and interpretation of RLCs for cultured benthic diatoms, errors which may equally apply for *in situ* measurements.

Methods

Navicula phyllepta *cultures*

Navicula phyllepta was obtained from the microalgal culture collection of the Laboratoire de Biologie Marine (ISOMer, Nantes, France). Stock cultures were grown in an artificial seawater medium (Harrison et al., 1980) at low irradiance (20 µmol photons m^{-2} s^{-1}, 6h/18h, light/dark photoperiod). The original medium was complemented following De Brouwer et al. (2002), with the addition of Fe-NH_4-citrate (1.37 µM final concentration), $CuSO_4$ $5H_2O$ (0.04 µM f.c.), folic acid (0.18 nM f.c.), nicotinic acid (0.0325 µM f.c.), thymine (0.95 µM f.c.), Ca-d-pantothenate (8.39 nM f.c.) and inositol (1.11 µM f.c.). Experiments were run with cultures grown in semi-continuous culture mode (volume: 250 mL, temperature: 15 ± 1°C) in Erlenmeyer flasks (500 mL) illuminated from below (100 µmol photons m^{-2} s^{-1},

14h/10h, light/dark photoperiod) by a high intensity discharge lamp (Osram HQI BT, 400 W).

Rapid light response curves

Fluorescence measurements were made using a Diving-PAM fluorimeter (Walz, Effeltrich, Germany). Sub-samples of *N. phyllepta* cultures were incubated at either low or high light (LL or HL; 25 or 400 µmol photons m^{-2} s^{-1} PPFD respectively), in a stirred, temperature controlled (15 °C) chamber, for 60 min. This light acclimation period was staggered, so that each sub-sample had been exposed for exactly 60 min prior to measurement of each RLC. After light acclimation, the culture sub-sample was transferred into a temperature controlled (15 °C) Hansatech DW2 chamber, with continuous stirring to prevent settling. The Diving-PAM fibre optic probe was applied to the top aperture of the chamber so that measurements were taken from cells exposed to the actinic light level applied from the halogen internal light source, thus minimising any light gradient effect (other apertures were darkened). Cultures were dark-adapted for 5 min prior to RLCs, with measurements at 10, 30 and 60 s at each light intensity. RLCs were performed with either incremental increases ('up') or decreases ('down') in the actinic light intensity between 0 and 1850 µmol photons m^{-2} s^{-1} PPFD. Light levels were measured using the Diving-PAM quantum meter, corrected against a calibrated Li-Cor LI-189 quantum meter with a Q21284 quantum sensor.

At each light level, effective photosystem II (PSII) quantum efficiency (F_q'/F_m', Oxborough et al. 2000; Lawson et al. 2002; Perkins et al. 2002) was measured by the saturation pulse technique, whereby a saturating light pulse of 7,600 µmol photons m^{-2} s^{-1} PPFD was applied for 400 ms to measure the maximum

fluorescence yield, F_m'. F_q'/F_m' is equivalent to $\Delta F/F_m'$ (Genty et al., 1989), however F_q' is preferred as it represents, not a change in fluorescence yield, but a difference resulting from photosynthetic quenching of yield, hence the suffix q (Oxborough et al., 2000). F_q'/F_m' was calculated as $(F_m' - F') / F_m'$, where F' is the fluorescence yield in the light adapted state, just prior to the application of the saturating pulse. Hence F_q'/F_m' is equivalent to the Genty parameter in the light adapted state (Genty et al. 1989). Relative electron transport rate (rETR) was then calculated as the product of F_q'/F_m' and PPFD/2 (Sakshaug et al. 1997; Perkins et al. 2001 2002).

The Diving-PAM has internal programmes allowing 8-step RLCs with increasing light levels. Therefore, RLCs were performed using the remote control functions in the WinControl software (Walz, Effeltrich, Germany) from a laptop computer, so as to apply decreasing as well as increasing light levels covering 12 light increments. This also enabled examination of the transient fluorescence kinetics, by monitoring the F' signal in the chart mode, allowing determination of F' 'steady-state' as well as examining changes in F' in response to application of each actinic light level.

Prior to all sets of light curves, the Diving-PAM auto-zero function was set using the Hansatech chamber filled with an equivalent volume of clear media. Light calibration was also carried out before and after all light curves due to an observed 10 % variation in halogen output over time, despite running the Diving-PAM from a mains supply. As a result light levels differed between curves by up to 10 %, with this variation accounted for in calculations of rETR.

Over-estimation of photochemical efficiency can occur when using the Diving-PAM with low biomass culture which results in an F' signal below 130 relative units (Walz Diving-PAM handbook). This low signal strength may also

177 occur at exposure to high light due to high levels of non-photochemical fluorescence
178 quenching (NPQ). Therefore the Diving-PAM gain setting was set to a maximum of
179 12 to avoid low values of *F'*. However at such a high gain, the auto-zero function can
180 also result in over-estimation of quantum efficiency. A large auto-zero value will be a
181 greater proportion of *F'* compared to F_m', when *F'* decreases as actinic light level
182 increases. Mathematically, the same percentage change in *F'* and F_m' will therefore
183 result in different values of F_q'/F_m' due to the weighted influence of the auto-zero.
184 Therefore, only measurements with a low auto-zero (< 40 relative units) were used in
185 the construction of RLCs.
186
187 *Non-sequential light response curves*
188
189 To remove the cumulative effect of light history experienced during a RLC, the above
190 methods were modified by using a different replicate sub-sample of culture for each
191 actinic light level. The range of light intensities was also extended up to 3200 µmol
192 photons m^{-2} s^{-1}. In addition a further RLC data point was added, with measurements
193 made when the fluorescence signal *F'* reached a constant level (as observed on the
194 Win Control software chart function). This value of *F'*, defined here as 'steady-state',
195 was probably not a true steady-state due to time limitations and so was not defined as
196 F_s.
197 Non-sequential light response curves (N-SLCs) and calculations were
198 otherwise the same as for rapid RLCs, except that a first set of curves used cells
199 maintained at 100 µmol photons m^{-2} s^{-1} PPFD, with no photo-acclimation to high or
200 low light. A second set of N-SLCs were then obtained using a different original semi-
201 continuous culture of *N. phyllepta*, but incorporating the HL and LL photoacclimation

period. These curves were not directly comparable to the preceding datasets, due to the change in source culture.

NPQ was calculated during N-SLCs, as ($F_m - F_m'$) / F_m' (Krause and Weiss 1991; Lavaud et al. 2002a). F_m' was measured as described above, using application of the saturating pulse after 10, 30 and 60 s at each irradiance, and when F' reached an approximate 'steady-state'. The maximum fluorescence yield in the dark adapted state, F_m, is more problematic to measure for diatoms, due to NPQ being maintained in the dark through processes such as chlororespiration (Jakob et al. 2001; Dijkman and Kroon 2002; Lavaud et al. 2002b), thus suppressing F_m below its true value (Mouget and Tremblin 2002). The calculated values of NPQ therefore show relative changes, using an approximation of F_m obtained after 5 min dark adaptation prior to each RLC.

Statistical analysis

RLCs of rETR against light intensity (PPFD) were constructed using the model of Eilers and Peeters (1988), estimating the maximum electron transport rate ($rETR_{max}$), the maximum light use efficiency (α) and the light saturation coefficient (E_k) calculated as ($rETR_{max}$ / α).

Curve fitting was achieved using the downhill simplex method of the Nelder-Mead model, and standard deviation of parameters was estimated by a bootstrap method under Fortan 77 code (Press et al. 2003). All fittings were tested by analyses of variance ($P<0.001$), residues being tested for normality and homogeneity of variance, and parameters significance by Student t-test ($P<0.05$). RLCs and

photosynthetic parameter comparisons were achieved using the method of Ratkowski (1983) for non-linear models.

Results

Rapid light response curves

Rapid RLCs for low light (LL) and high light (HL) acclimated cultures of *N. phyllepta* showed saturation and down regulation when irradiance was reduced from 1850 µmol photons m^{-2} s^{-1} (Fig. 1A,B: 10, 30 and 60 down). In contrast, when irradiance was incrementally increased, light saturation and photoinhibition (Fig. 1A,B: 10, 30 and 60 up) did not occur. When irradiance was increased or reduced, rETR above 500 µmol photons m^{-2} s^{-1} increased in proportional to the increase in length of time at each light level.

Calculated values of $rETR_{max}$, α and E_k obtained from RLCs with decreasing light levels were compared between HL and LL cultures (Fig. 2). 10, 30 and 60 s RLCs for HL cultures showed $rETR_{max}$ and E_k higher and α lower than LL cultures ($P<0.001$; Fig. 2A,B,C). Thus photoacclimation occurred within the 1 h light treatment period. $rETR_{max}$ increased significantly with the length of irradiance step for low light and high light ($P < 0.01$) acclimated cultures, whereas α showed no significant correlation with length of irradiance step. E_k, due the nature of its derivation from ($rETR_{max}$ / α) showed the same increase as $rETR_{max}$ as a function of lengthening irradiance step ($P<0.001$).

RLCs with increasing light levels did not saturate for LL (Fig. 1A: 60 s) and HL cultures (Fig. 1B: 10, 30 and 60 s), preventing calculation of $rETR_{max}$ and E_k. Estimation of α indicated photoacclimation patterns similar to the decreasing

irradiance RLCs. LL cultures had significant higher values of α compared to HL cultures ($P<0.001$). 10 and 30 s LCRs for LL cultures just reached saturation, and showed the same pattern in $rETR_{max}$ observed for decreasing RLCs, with a significant increase in $rETR_{max}$ (165 to 235 rel. units from 10 to 30 s respectively), an increase in E_k (319 to 439 µmol photons m^{-2} s^{-1} PPFD), but no change in α (0.52 rel. units).

Non-sequential light response curves

Separate replicate *N. phyllepta* cultures used for each light level (Fig. 3) resulted in N-SLCs with similar patterns as rapid RLCs (Fig. 1). rETR increased significantly with length of irradiance step ($P <0.001$) at irradiances above 300 µmol photons m^{-2} s^{-1}, with correspondingly higher $rETR_{max}$. 10, 30 and 60 s RLCs all showed light saturation and down regulation, whereas light curves when *F'* was allowed to reach an apparent 'steady-state' at each light intensity, did not saturate. No steady state data point was possible at 1850 µmol photons m^{-2} s^{-1} as photosynthetic down regulation (presumably NPQ) resulted in a Chl *a* fluorescence yield (*F'*) below the minimum value of 130 relative units required for accurate measurement of F_q'/F_m'.

N. phyllepta (a different culture from that used above and so not directly comparable) was then acclimated to either low (25 µmol photons m^{-2} s^{-1}) or high (400) light as above, prior to RLCs with different replicate cultures used for each light intensity (Fig. 4). There were significant differences between the curves ($P<0.001$), HL and LL cultures showed a significant increase in rETR proportional to an increase in time at each irradiance step, except between 10 and 30 s HL, 30 and 60 s HL and between steady state HL and LL RLCs.

Despite changing replicate cultures for each light level, the same patterns were observed as for the rapid RLCs (Fig. 1). HL acclimated cultures had significant greater $rETR_{max}$ ($P<0.001$, Fig. 5A), and higher E_k ($P<0.001$, Fig. 5C) than LL acclimated cultures. There were no significant differences for α ($P>0.05$; Fig. 5B). However the difference in $rETR_{max}$ between HL and LL cells declined as the time at each RLC increment increased. There was a significant increase in $rETR_{max}$ and E_k with the length of irradiance step for low light and high light acclimated cultures ($P<0.001$); α showed no significant differences for both LL and HL cultures ($P>0.05$).

Chl a fluorescence and NPQ kinetics

An example of the fluorescence kinetics obtained at irradiance steps above 300 µmol photons m^{-2} s^{-1} is reproduced (Fig. 6) showing the position at which saturation pulses were applied. The example is for a low-light culture (25 µmol m^{-2} s^{-1}), transferred to 370 µmol m^{-2} s^{-1}. At 10 s the comparatively slow data acquisition time of the Diving-PAM fluorimeter (compared to the rapid induction of fluorescence quenching) resulted in an under-estimation of F_q'/F_m'. This resulted from the high rate of decrease in F' following the increase in actinic irradiance. F' was recorded by the Diving-PAM prior to a further decrease before the measurement of F_m'. F' and F_m' were therefore recorded at different times, resulting in under-estimation of F_m' relative to F' so that values of F_q'/F_m' were underestimated and often values of zero were reported. 10 s light curves would then result in under-estimation of rETR above 300 µmol photons m^{-2} s^{-1} PPFD. This was most obvious for HL cultures, which showed a more rapid decline in F' compared to LL cultures (data not shown). The magnitude of the increase in F' on the application of the actinic light and the rate of

decline after the peak in *F'* both increased as irradiance increased above 300 µmol photons m^{-2} s^{-1}.

Above 300 µmol photons m^{-2} s^{-1}, NPQ was induced rapidly during RLCs, with relatively high levels after 60 s at each irradiance, for both LL and HL acclimated cultures (Fig. 7). While the amplitude of NPQ increased with illumination time for LL cultures, it remained relatively similar for HL cultures. LL cultures (Fig. 7A) had similar or lower levels of NPQ compared to HL cultures (Fig. 7B) after 10, 30 and 60 s, but higher NPQ at 'steady-state' (insert, Fig. 7B).

Discussion

The aims of the study were to determine the effects of light history prior to, and accumulated light dose during, a light response curve (RLC) obtained using Chl *a* fluorescence. It was expected that the light dose experienced by the algal cells over different time scales during RLCs, would affect the Chl *a* fluorescence measurements obtained, and hence modify the resulting RLCs and photophysiological parameters derived. The data obtained raise important questions with regard to the measurement and interpretation of Chl *a* fluorescence rapid RLCs. The primary question is, what is being measured for light curves of different length of actinic irradiance steps?

The data reported here suggest two stages of photoacclimation. Firstly, the acclimation resulting from exposure to low and high irradiance prior to RLCs, effectively the type of photoacclimation that a RLC attempts to detect. Secondly, the 'acclimation' during the RLCs themselves; which RLC methodology should avoid. In addition, the limitations of available methodology must also be considered.

The effect of accumulated light dose on RLCs interpretation

RLCs with incremental decreases in irradiance showed saturation and a decrease in $rETR_{max}$ at higher irradiance due to photoinhibition (Fig. 1). In contrast, RLCs with increasing irradiance often did not saturate. This raises the first issue of RLCs methodology: the effect of accumulated light dose during the light curve, dependent upon the order of irradiances ('up' or 'down') and the duration of each step (from 10 s to 2-3 min).

With increasing irradiance, there is an accumulative effect of light dosage resulting in progressive induction, occurring on a time scale of 10's of seconds, of the different components of the photosynthetic apparatus. Ubiquinone (Q_A) oxidation, the rate limiting step in electron transport (Dau 1994) would have been faster for increasing irradiance light curves due to induction of more rapid photochemical energy transfer. Also, induction of non-photochemical Chl *a* fluorescence quenching, NPQ will have increased proportionally to the light dose experienced during the RLC. In diatoms, the photosynthetic translocation of protons across the thylakoid membrane has been linked to energy dependent NPQ (Ting & Owens 1993; Lavaud et al. 2002c) associated with xanthophyll pigment synthesis (Arsalane et al. 1994; Olaizola et al. 1994; Lavaud et al. 2002a 2003 2004; Serôdio et al. 2005b). This process generates a photoprotective dissipation of excess energy in photosystem II (PSII) reducing the Chl *a* fluorescence yield, on a time scale of 10's of seconds (MacIntyre et al. 2000; Lavaud et al. 2002a 2004; Raven and Geider 2003). Hence, Q_A oxidation and NPQ will affect in complex ways, the measurement of effective PSII quantum efficiency and resultant calculation of (r)ETR.

Increasing the duration of each incremental irradiance step was also seen to induce photoacclimation. As the length of each step increased from 10 to 60 s rETR increased proportionally, often resulting in a lack of saturation for RLCs with increasing irradiance. Above 500 µmol photons m^{-2} s^{-1}, NPQ increased in importance, and the duration for each irradiance step increased the extent of NPQ (Fig. 7). In *N. phyllepta,* Q_A oxidation was the primary cause of the change in fluorescence yield for RLCs with 10 s steps, however for 30 s and above, the level of NPQ became most significant. As discussed below, the relative importance of Q_A oxidation and NPQ is species and light history dependent, and in diatoms the relationship between PSII redox-state and NPQ is species specific (Ruban et al. 2004; Lavaud unpublished results).

For decreasing irradiance steps, the accumulative light dose effect described above was reduced relative to increasing irradiance RLCs. However, decreasing the irradiance and hence immediate exposure to high irradiance did not appear to induce photodamage. Two observations support this, the low amplitude of NPQ for 10 and 30 s illumination duration at high irradiances, and the fact that rETR below 500 µmol photons m^{-2} s^{-1} was similar to that obtained with increasing irradiance. The use of decreasing irradiance therefore reduces the over-estimation of rETR and is likely to be more representative of the photophysiological state of the diatom cells prior to application of the RLC, which is the state that the RLC aims to ascertain.

Despite changing the culture used for each irradiance step (N-SLCs), the same patterns in data were observed as for rapid RLCs (Fig. 3, 4). rETR increased as a function of the length of irradiance during the light curve, such that even when *F'* was allowed to reach an approximation of 'steady-state', RLCs failed to saturate. The N-SLCs indicate that the effect of light dose on the fluorescence measurements occurred

rapidly, within the duration of each irradiance step. This observation confirms the impact of combined Q_A redox state and NPQ on the Chl *a* fluorescence kinetics and acquisition of *F'* and *Fm'* for the calculation of rETR (see Fig. 6).

Ralph and Gademann (2005) conducted a recent similar investigation on the higher aquatic plant *Zostera marina*. They did not report a lack of saturation of the rETR curves, but in some cases did report a lack of down regulation post saturation. This lack of down regulation occurred for plants after low light treatment, and Ralph and Gademann (2005) suggested that their capacity for down regulation was exceeded. This differs from the data reported in the present study, where a lack of saturation in rETR was greater for high light compared to low light treatments, despite a higher capacity for NPQ in the former. We suggest that the lack of saturation of RLCs observed with *N. phyllepta* is an additional indication (see also Ruban et al. 2004) that rapid photoacclimatory processes occur in diatoms which can greatly affect fluorescence measurements, and especially the velocity of fluorescence transients (Ruban et al. 2004). Rapid processes known to occur to a higher extent and with more rapid induction kinetics in diatoms are the xanthophyll cycle (Jakob et al 2001; Lavaud et al 2004), NPQ (Lavaud et al. 2002a; Ruban et al 2004, Serôdio et al. 2005b) and the PS II electron cycle (Lavaud et al 2002b).

The effect of light history on RLC interpretation

The effects of the order and the duration of each RLC irradiance step were greatest for high light (HL) acclimated cultures (Fig. 1, 4). The light history, to which the cells were exposed, modified the speed of response of photochemistry to short changes in irradiance. HL cells had a greater capability to respond quickly to an increase in

irradiance, most likely due to a greater availability in electron acceptors from photochemical reactions, increasing the speed of Q_A oxidation. The more rapid kinetics for NPQ in HL cells can be explained by the basal level of NPQ developed after 1 h exposure at 400 µmol photons m^{-2} s^{-1}, which did not relax during the 5 min dark adaptation (Lavaud et al. 2002c; Ruban et al. 2004) In diatoms, NPQ amplitude and kinetics are closely related to the amount of xanthophylls (Casper-Lindley and Bjorkman 1998; Lavaud et al. 2002a 2002c), and are dependent upon light history (Willemoes and Monas 1991; Mouget et al. 1999 2004; Lavaud et al. 2003), the state of growth (Arsalane et al. 1994) and the species (Lavaud et al. 2004; Serôdio et al. 2005b). Thus, all these aspects have to be taken into account in the potential effects of NPQ during the RLC acquisition and interpretation.

Consequences for photophysiological parameters calculated from the RLCs

An expected pattern was observed when comparing $rETR_{max}$, α and E_k between HL and LL cultures (Fig. 2). The 1 h acclimation resulted in higher $rETR_{max}$ and E_k and lower α for HL compared to LL cells. Higher $rETR_{max}$ and E_k are typical for high light acclimated cells which have modified their light harvesting to utilise the high levels of light to which they are exposed. Conversely, low light acclimated cells modify their photophysiology to maximise light harvesting efficiency and hence have higher values of α. However the light dose effect experienced during the RLCs reduced or even negated these differences in $rETR_{max}$. Similarly, for N-SLCs, the differences in photophysiological parameters reduced as a function of increasing length of each irradiance period. As a result, no difference was observed in $rETR_{max}$ by ‘steady-state’ (Fig. 5). This implies that long irradiance steps caused a photo-dose

effect that reduced or even negated the real level of 1 h photoacclimation. It remains surprising though that cultures of *N. phyllepta* acclimated to 25 or 400 µmol photons m^{-2} s^{-1} did not saturate at 1850 µmol photons m^{-2} s^{-1}. *N. phyllepta* may have a high capacity to respond quickly to high light, probably through regeneration of ADP and $NADP^+$ and as a result of alternative electron pathways known to be active in diatoms (Caron et al. 1987; Lavaud et al. 2002b; Wilhelm et al. 2004). This is possibly a common feature of benthic diatoms, which may often experience rapid variations in incident light intensity.

Although the dataset was obtained from measurements on diatom cells in culture, the data suggest possible ecological implications with regard to diatom acclimation to light environment fluctuation *in situ* (Serôdio et al. 2005b). It would appear that *N. phyllepta* has a high ability to acclimate quickly to increasing irradiance. This would obviously be an advantage to cells inhabiting an open mudflat environment in which rapid changes could occur, e.g. as a result of cloud induced light flecking. Any energy dependent photoprotective acclimation, being more rapid than downward migration, would not only precede migration (Underwood et al., 2005) should high irradiance persist, but would also prevent wasteful short-term migrations requiring production and excretion of extracellular polymeric substances (carbohydrates generically described as EPS) used in migration (Consalvey et al. 2005b and references there-in).

Specificity of the RLCs acquisition with the Diving-PAM methodology

Analysis of the fluorescence kinetics from *N. phyllepta* indicated an aspect of methodology, which may be particular to the Diving-PAM, and which can generate an

error in the measurement of F_m' and hence rETR for 10 s irradiance steps (see the description in the Results section, Fig. 6). To summarise, the time delay between measurement of F' and the corresponding F_m' used in calculation of the quantum efficiency resulted (during this study) in an under-estimation of F_m' relative to F' and hence a falsely low efficiency. The example illustrated was for a low light culture at 25 μmol m^{-2} s^{-1}, transferred to 370 μmol m^{-2} s^{-1}. This is an abrupt change, however the effect was greatest for HL acclimated cultures and at high irradiances, when the rate decay in F' (presumably resulting from interaction between Q_A oxidation and NPQ induction) was greatest. As such the level of this error is a function of light dose and hence the light history to which the cells were exposed. This problem was not encountered with the higher aquatic plant *Zostera* (Ralph and Gademann 2005) presumably because the transients in fluorescence yield in plants are slower than in diatoms, although NPQ relaxation is slower in diatoms (Ruban et al. 2004).

Conclusions

The present work indicates that light dose and light history strongly affect fluorescence measurements used in RLC acquisition. These features have to be taken into account in the acquisition and interpretation of Chl *a* fluorescence RLCs. For cultured benthic diatoms, and presumably for *in situ* mixed biofilms for the same reasons, extreme care should be taken in choice of light curve methodology. Parameters measured will be functions of light history and light exposure during the light curve itself and the extent of this will in turn be dependent upon the light history prior to the RLC. It is suggested that it is not always possible to answer the question posed above: what is being measured for light curves of different length of actinic irradiance? It is not possible to extrapolate these results to make general comments for

all diatom species, nor to say that the changes suggested will occur for *in situ* measurements. Indeed, no methodology is perfect and in many cases measurement itself induces a change, thus making the commonly stated "non-intrusive" nature of fluorescence measurements incorrect. For example, an increasing RLC induces photoacclimation, however a decreasing RLC will allow dissipation of photophysiological state (e.g. high light induced NPQ) as light level is reduced: neither method is devoid of experimental error. However it is suggested that the changes induced during a RLC should be carefully considered during interpretation of results. In general, RLCs of 60 s or those with increasing incremental irradiance steps may not detect differences in photophysiological state caused by light history, differences that RLCs aim to determine. Conversely RLCs with short irradiance steps may result in errors due to rapid NPQ induction and Q_A oxidation, especially for diatom cells exposed to high light or a high-accumulated light dose history. Overall, re-programming of the Diving-PAM fluorimeter to enable RLCs with decreasing irradiance levels is advised, and RLCs of 30 s at each irradiance step may be optimal for use with benthic diatoms.

494 **References**

495 Arsalane W, Rousseau B, Duval J-C (1994) Influence of the pool size of the
496 xanthophyll cycle on the effects of light stress in a diatom: competition between
497 photoprotection and photoinhibition. Photochem Photobiol 60: 237–243

498

499 Barranguet C, Kromkamp J (2000) Estimating primary production rates from
500 photosynthetic electron transport in estuarine microphytobenthos. Mar Ecol Prog Ser
501 204: 39–52

502

503 Casper-Lindley C, Björkman O (1998) Fluorescence quenching in four unicellular
504 algae with different light-harvesting and xanthophyll-cycle pigments. Photosynth Res
505 56: 277–289

506

507 Caron L, Berkaloff C, Duval J-C, Jupin H (1987) Chlorophyll fluorescence transients
508 from the diatom *Phaeodactylum tricornutum*: relative rates of cyclic phosphorylation
509 and chlororespiration. Photosynth Res 11: 131–139

510

511 Consalvey M, Jesus B, Perkins RG, Brotas V, Underwood GJC, Paterson DM (2004)
512 Monitoring migration and measuring biomass in benthic biofilms: the effects of
513 dark/far-red adaptation and vertical migration on fluorescence measurements.
514 Photosynth Res 81: 91–101

515

516 Consalvey M, Perkins RG, Paterson DM, Underwood GJC (2005a) PAM
517 fluorescence: a beginners guide for benthic diatomists. Diatom Res 20: 1–22

518

519 Consalvey M, Paterson DM, Underwood GJC (2005b) The ups and downs of life in a
520 benthic biofilm: migration of benthic diatoms. Diatom Res 19 :181-202
521
522 Dau H (1994) Molecular mechanisms and quantitative models of variable
523 photosystem II fluorescence. Photochem Photobiol 60: 1–23
524
525 De Brouwer JFC, Wolfstein K, Stal LJ (2002) Physical characterization and diel
526 dynamics of different fractions of extracellular polysaccharides in an axenic culture of
527 a benthic diatom. Eur J Phycol 37: 37–44
528
529 Demers S, Roy S, Gagnon R, Vignault C (1991) Rapid light-induced changes in cell
530 fluorescence and in xanthophyll-cycle pigments of *Alexandrium excavatum*
531 (Dinophyceae) and *Thalassiosira pseudonana* (Bacillariophyceae): a photo-protection
532 mechanism. Mar Ecol Prog Ser 76: 185–193
533
534 Dijkman NA, Kroon BMA (2002) Indications for chlororespiration in relation to light
535 regime in the marine diatom *Thalassiosira weissflogii*. J Photochem Photobiol B 66:
536 179–187
537
538 Eilers PHC, Peeters JCH (1988) A model for the relationship between light intensity
539 and the rate of photosynthesis in phytoplankton. Ecol Model 42: 199-215
540
541 Flameling IA, Kromkamp J (1998) Light dependence of quantum yields for PSII
542 charge separation and oxygen evolution in eucaryotic algae. Limnol Oceanogr 43:
543 284–297
544

545 Genty B, Briantais JM, Baker NR (1989) The relationship between the quantum yield
546 of photosynthetic electron transport and quenching of chlorophyll fluorescence.
547 Biochim Biophys Acta 990: 87–92
548
549 Gévaert F, Créach A, Davoult D, Migné A, Levavasseur G, Arzel P, Holl A-C,
550 Lemoine Y (2003) *Laminaria saccharina* photosynthesis measured in situ:
551 photoinhibition and xanthophyll cycle during a tidal cycle. Mar Ecol Prog Ser 247:
552 43–50
553
554 Glud RN, Kühl M, Wenzhöfer F, Rysgaard S (2002) Benthic diatoms of a high Arctic
555 fjord (Young Sound, NE Greenland): importance for ecosystem primary production.
556 Mar Ecol Prog Ser 238: 15–29
557
558 Harker M, Berkaloff C, Lemoine Y, Britton G, Young AJ, Duval J-C, Rmiki N-E,
559 Rousseau B (1999) Effects of high light and desiccation on the operation of the
560 xanthophyll cycle in two marine brown algae. Eur J Phycol 34: 35–42
561
562 Harrison PJ, Waters RE, Taylor FJR (1980) A broad spectrum artificial seawater
563 medium for coastal and open ocean phytoplankton. J Phycol 16: 28–35
564
565 Hartig P, Wolfstein K, Lippemeier S, Colijn F (1998) Photosynthetic activity of
566 natural microphytobenthos populations measured by fluorescence (PAM) and ^{14}C-
567 tracer methods: a comparison. Mar Ecol Prog Ser 166: 53–62
568

569 Honeywill C, Paterson DM, Hagerthey SE (2002) Determination of
570 microphytobenthic biomass using pulse amplitude modulated minimum fluorescence.
571 Eur J Phycol 37: 485–492
572
573 Jakob T, Goss R, Wilhelm C (2001) Unusual pH-dependence of diadinoxanthin de-
574 epoxidase activation causes chlororespiratory induced accumulation of diatoxanthin in
575 the diatom *Phaeodactylum tricornutum*. J Plant Physiol 158: 383–390
576
577 Kromkamp J, Barranguet C, Peene J (1998) Determination of microphytobenthos
578 PS II quantum efficiency and photosynthetic activity by means of variable chlorophyll
579 fluorescence. Mar Ecol Prog Ser 162: 45–55
580
581 Kühl M, Glud RN, Borum J, Roberts R, Rysgaard S (2001) Photosynthetic
582 performance of surface-associated algae below sea ice as measured with a pulse-
583 amplitude modulated (PAM) fluorometer and O_2 microsensors. Mar Ecol Prog Ser
584 223: 1–14
585
586 Lavaud J, Rousseau B, van Gorkom HJ, Etienne A-L (2002a) Influence of the
587 diadinoxanthin pool size on photoprotection in the marine planktonic diatom
588 *Phaeodactylum tricornutum*. Plant Physiol 129: 1398–1406
589
590 Lavaud J, van Gorkom HJ, Etienne A-L (2002c) Photosystem II electron transfer
591 cycle and chlororespiration in planktonic diatoms. Photosynth Res 74: 51–59
592

593 Lavaud J, Rousseau B, Etienne A-L (2002c) In diatoms, a transthylakoid proton
594 gradient alone is not sufficient to induce a non-photochemical fluorescence
595 quenching. FEBS Letters 523: 163–166
596
597 Lavaud J, Rousseau B, Etienne A-L (2003) Enrichment of the light-harvesting
598 complex in diadinoxanthin and implications for the non-photochemical fluorescence
599 quenching in diatoms. Biochem 42: 5802–5808
600
601 Lavaud J, Rousseau B, Etienne A-L (2004) General features of photoprotection by
602 energy dissipation in planktonic diatoms (Bacillariophyceae). J Phycol 40: 130–137
603
604 Lawson T, Oxborough K, Morrison JIL, Baker NR (2002) Responses of
605 photosynthetic electron transport in stomatal guard cells and mesophyll cells in intact
606 leaves to light, CO_2, and humidity. Plant Physiol 128: 52–62
607
608 MacIntyre HL, Geider RJ, Miller DC (1996) Microphytobenthos: The ecological role
609 of the 'secret garden' of unvegetated, shallow-water marine habitats. I-Distribution,
610 abundance and primary production.
611
612 MacIntyre HL, Kana TM, Geider RJ (2000) The effect of water motion on short-term
613 rates of photosynthesis by marine phytoplankton. Trends Plant Sci 5: 12–17
614
615 Mouget J-L, Tremblin G, Morant-Manceau A, Morançais M, Robert J-M (1999)
616 Long-term photoacclimation of *Haslea ostrearia* (Bacillariophyta): effect of

617 irradiance on growth rates, pigment content and photosynthesis. Eur J Phycol 34:
618 109–115
619
620 Mouget J-L, Tremblin G (2002) Suitability of the Fluorescence Monitoring System
621 (FMS, Hansatech) for measurement of photosynthetic characteristics in algae. Aquat
622 Bot 74: 219–231
623
624 Mouget J-L, Rosa P, Tremblin G (2004) Acclimation of *Haslea ostrearia* to light of
625 different spectral qualities – Confirmation of 'chromatic adaptation' in diatoms. J
626 Photoch Photobio B 75: 1–11
627
628 Olaizola M, Laroche J, Kolber Z, Falkowski PG (1994) Non-photochemical
629 fluorescence quenching and the diadinoxanthin cycle in a marine diatom. Photosynth
630 Res 41: 357–370
631
632 Oxborough K, Hanlon ARM, Underwood GJC, Baker NR (2000) An instrument
633 capable of imaging chlorophyll a fluorescence from intact leaves at very low
634 irradiance and at cellular and subcellular levels of organization. Plant Cell Environ 20:
635 1473–1483
636
637 Perkins RG, Underwood GJC, Brotas V, Snow G, Jesus B, Ribeiro L (2001) *In situ*
638 microphytobenthic primary production during low tide emersion in the Tagus estuary,
639 Portugal: production rates, carbon partitioning and vertical migration. Mar Ecol Prog
640 Ser 223: 101–112
641

642 Perkins RG, Oxborough K, Hanlon ARM, Underwood GJC, Baker NR (2002) Can
643 chlorophyll fluorescence be used to estimate the rate of photosynthetic electron
644 transport within microphytobenthic biofilms? Mar Ecol Prog Ser 228: 47–56
645
646 Press WH, Teukolsky SA, Vetterling WT, Flannery BP (2003) Numerical recipes in
647 Fortran 77: The art of scientific computing. Cambridge University press, 933 pp
648
649 Ralph PJ, Gademann R, Larkum AWD, Schreiber U (1999) *In situ* underwater
650 measurements of photosynthetic activity of coral zooanthellae and other reef-dwelling
651 dinoflagellate endosymbionts. Mar Ecol Prog Ser 180: 139–147
652
653 Ralph PJ, Gademann R (2005) Rapid light curves: A powerful tool to assess
654 photosynthetic activity. Aquat Bot 82: 222-237
655
656 Ratkowski DA (1983) Non linear regression modeling. A unified practical approach.
657 Marcal Dekker INC., New-York, 276 pp
658
659 Raven JA, Geider RJ (2003). Adaptation, acclimation and regulation in algal
660 photosynthesis. In: Larkum AWD, Douglas S, Raven JA (eds) Photosynthesis in
661 Algae. Adv Photosynth Res 17, Kluwer Dordrecht, pp 385–412
662
663 Rodrigues MA, dos Santos CP, Young AJ, Strbac D, Hall DO (2002) A smaller and
664 impaired xanthophyll cycle makes the deeps sea macroalgae *Laminaria abyssalis*
665 (Phaeophyceae) highly sensitive to daylight when compared with shallow water
666 *Laminaria digitata*. J Phycol 38: 939-947
667

668 Ruban AV, Lavaud J, Rousseau B, Guglielmi G, Horton P, Etienne A-L (2004) The
669 super-excess energy dissipation in diatom algae: comparative analysis with higher
670 plants. Photosynth Res 82: 165 – 175
671
672 Sakshaug E, Bricaud A, Dandonneau Y, Falkowski P, Keifer D, Legendre L, Morel
673 A, Parslow J, Takahashi M (1997) Parameters of photosynthesis: definitions, theory
674 and interpretation of results. J Plankton Res 19:1637–1670
675
676 Schreiber U, Schliwa U, Bilger W (1986) Continuous recording of photochemical
677 chlorophyll fluorescence quenching with a new type of modulation fluorometer.
678 Photosynth Res 10: 51–62
679
680 Schreiber U, Gademann R, Ralph PJ, Larkum AWD (1997) Assessment of
681 photosynthetic performance of *Prochloron* in *Lissoclinum patella* in hospite by
682 chlorophyll fluorescence measurements. Plant Cell Physiol 38: 945–951
683
684 Serôdio J, da Silva JM, Catarino F (1997) Non-destructive tracing of migratory
685 rhythms of intertidal benthic microalgae using *in vivo* chlorophyll *a* fluorescence. J
686 Phycol 33: 542–553
687
688 Serôdio J, Catarino F (2000) Modelling the primary productivity of intertidal
689 microphytobenthos: time scales of variability and effects of migratory rhythms. Mar
690 Ecol Prog Ser 192: 13–30
691

692 Serôdio J (2003) A chlorophyll fluorescence index to estimate short-term rates of
693 photosynthesis by intertidal microphytobenthos. J Phycol 39: 33–46
694
695 Serôdio J, Viera S, Cruz S, Barroso F (2005a) Short-term variability in the
696 photosynthetic activity of microphytobenthos as detected by measuring light curves
697 using variable fluorescence. Mar Biol 146: 903-914
698
699 Serôdio J, Cruz S, Viera S and Brotas V (2005b) Non-photochemical quenching of
700 chlorophyll fluorescence and operation of the xanthophyll cycle in estuarine
701 microphytobenthos. J Exp Mar Biol Ecol in press
702
703 Ting CS, Owens TG (2003) Photochemical and non-photochemical fluorescence
704 quenching processes in the diatom *Phaeodactylum tricornutum*. Plant Physiol
705 101:1323-1330
706
707 Underwood GJC, Perkins RG, Consalvey MC, Hanlon ARM, Baker NR, Paterson
708 DM (2005) Patterns in microphytobenthic primary productivity: Species-specific
709 variation in migratory rhythms and photosynthesis in mixed-species biofilms. Limnol
710 Oceanogr 50: 755-767
711
712 Underwood GJC, Kromkamp J (1999) Primary production by phytoplankton and
713 microphytobenthos in estuaries, p. 93-153. In Nedwell DB, Raffaelli DG (eds.)
714 Advances in Ecological Research: Estuaries 29. Academic Press, San Diego, USA
715
716

717 Wilhelm C, Becker A, Toepel J, Vieler A, Rautenberger R (2004) Photophysiology
718 and primary production of phytoplankton in freshwater. Physiol Plantarum 120: 347–
719 357

720

721 Willemoës M, Monas E (1991) Relationship between growth irradiance and the
722 xanthophyll cycle pool in the diatom *Nitzschia palea*. Physiol Plantarum 83: 449–456

723

724

725 **Figure Legends**

726

727 Figure 1. Rapid light response curves for *N. phyllepta* cultures grown at an irradiance
728 of 100 µmol photons m^{-2} s^{-1} and exposed to 1 h light acclimation period of low (A, 25
729 µmol photons m^{-2} s^{-1}) or high (B, 400 µmol photons m^{-2} s^{-1}) light. Light response
730 curves were run with irradiance durations at each light curve increment of 10, 30 and
731 60 s and with either increasing (up) or decreasing (down) irradiance steps. Curves
732 were constructed using the model of Eilers and Peeters (1988) followed by curve
733 fitting following the Nelder-Mead model (Press et al., 2003).

734

735 Figure 2. Rapid light response curve parameters for light curves obtained using
736 decreasing irradiance steps, shown in Fig. 1. (A) maximum electron transport rate,
737 $rETR_{max}$; (B) maximum light use coefficient (α); (C) light saturation coefficient (E_k).

738

739 Figure 3. Non-sequential light response curves for *N. phyllepta* cultures grown at 100
740 µmol photons m^{-2} s^{-1}. Light curves were run using different sub-samples of culture for
741 each light curve step and with irradiance durations of 10, 30 and 60 s, followed by a
742 final measurement when *F'* reached approximate 'steady-state' after 2 to 3 minutes.
743 Curves were constructed using the model of Eilers and Peeters (1988) followed by
744 curve fitting following the Nelder-Mead model (Press et al., 2003).

745

746 Figure 4. Non-sequential light response curves (mean ± s.e., n = 3) for *N. phyllepta*
747 cultures grown at an irradiance of 100 µmol photons m^{-2} s^{-1} and exposed to 1 h light
748 acclimation period of low (A, 25 µmol photons m^{-2} s^{-1}) or high (B, 400 µmol photons
749 m^{-2} s^{-1}) light. Light curves were run using different sub-samples of culture for each
750 light curve step, and with irradiance durations of 10, 30 and 60 s, followed by a final

751 measurement when *F'* reached approximate 'steady-state' after 2 to 3 minutes. Curves
752 were constructed using the model of Eilers and Peeters (1988) followed by curve
753 fitting following the Nelder-Mead model (Press et al., 2003).
754
755 Figure 5. Non-sequential light response curve parameters (mean ± s.e., n = 3) for
756 light curves obtained using different sub-samples of *N. phyllepta* culture for each
757 irradiance step, shown in Figure 4. (A) maximum electron transport rate, $rETR_{max}$; (B)
758 maximum light use coefficient (α); (C) light saturation coefficient (E_k).
759
760 Figure 6. Example of fluorescence kinetics obtained for a sub-sample of *N. phyllepta*
761 low-light culture used in a non-sequential light response curve step. Application of
762 saturating pulses are indicated by downward arrows after 10, 30 and 60 s and when *F'*
763 reached approximate 'steady-state' after 2 to 3 minutes. The actinic light increase was
764 from 25 to 370 µmol m^{-2} s^{-1}.
765
766 Figure 7. Non-photochemical Chl *a* fluorescence quenching (NPQ) calculated as (F_m -
767 F_m') / F_m' for non-sequential light curves (Fig. 4) of *N. phyllepta* exposed to 1 h light
768 acclimation period of low (A, 25 µmol photons m^{-2} s^{-1}) or high (B, 400 µmol photons
769 m^{-2} s^{-1}) light. NPQ was calculated using F_m' obtained from saturating pulses after
770 irradiance durations of 10, 30 and 60 s, followed by a final measurement when *F'*
771 reached approximate 'steady-state' after 2 to 3 minutes. The insert shows the change
772 in NPQ at 560 and 3200 µmol photons m^{-2} s^{-1} over time.
773
774
775

776

Figure 1

777
778
779

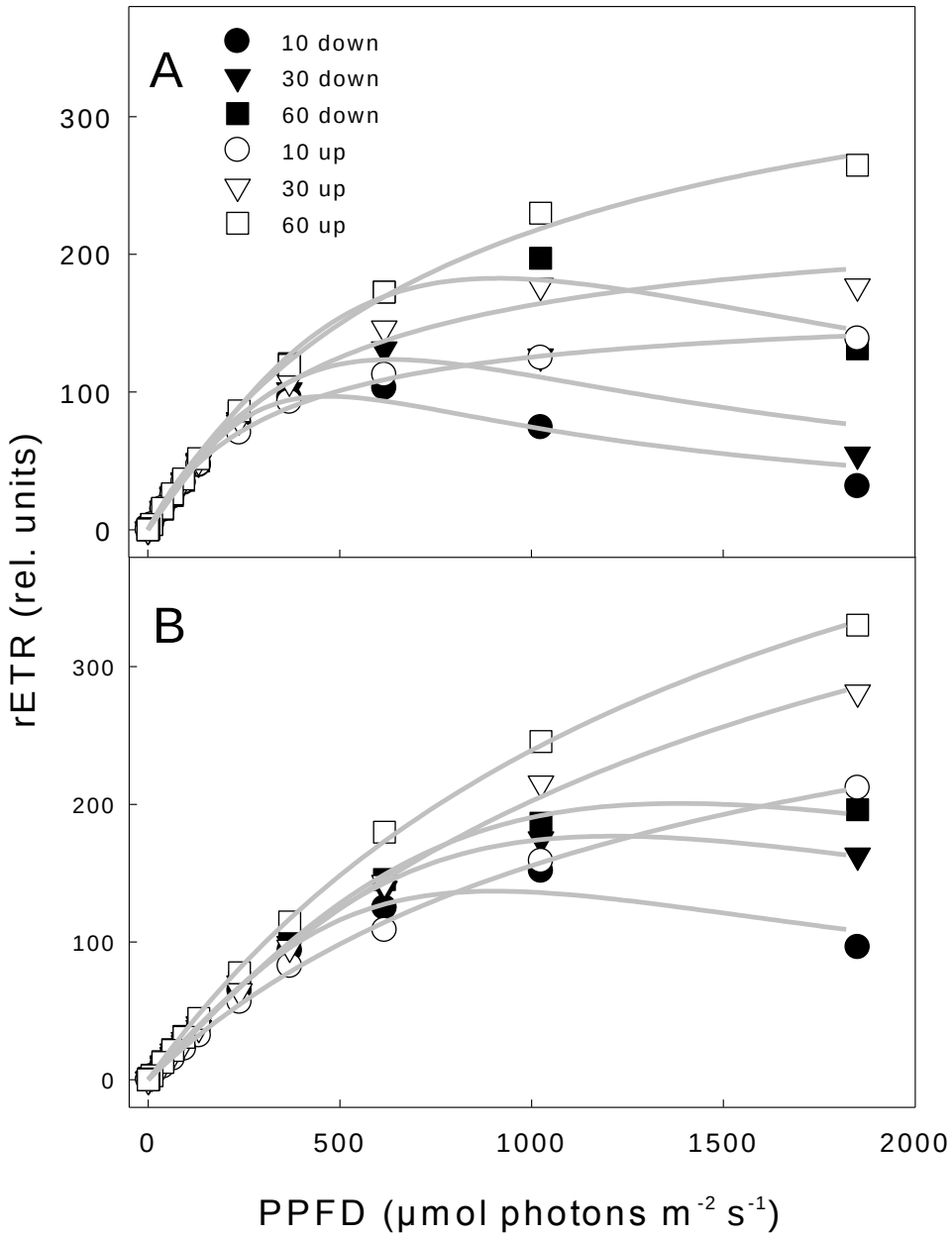

780

781

782

Figure 2

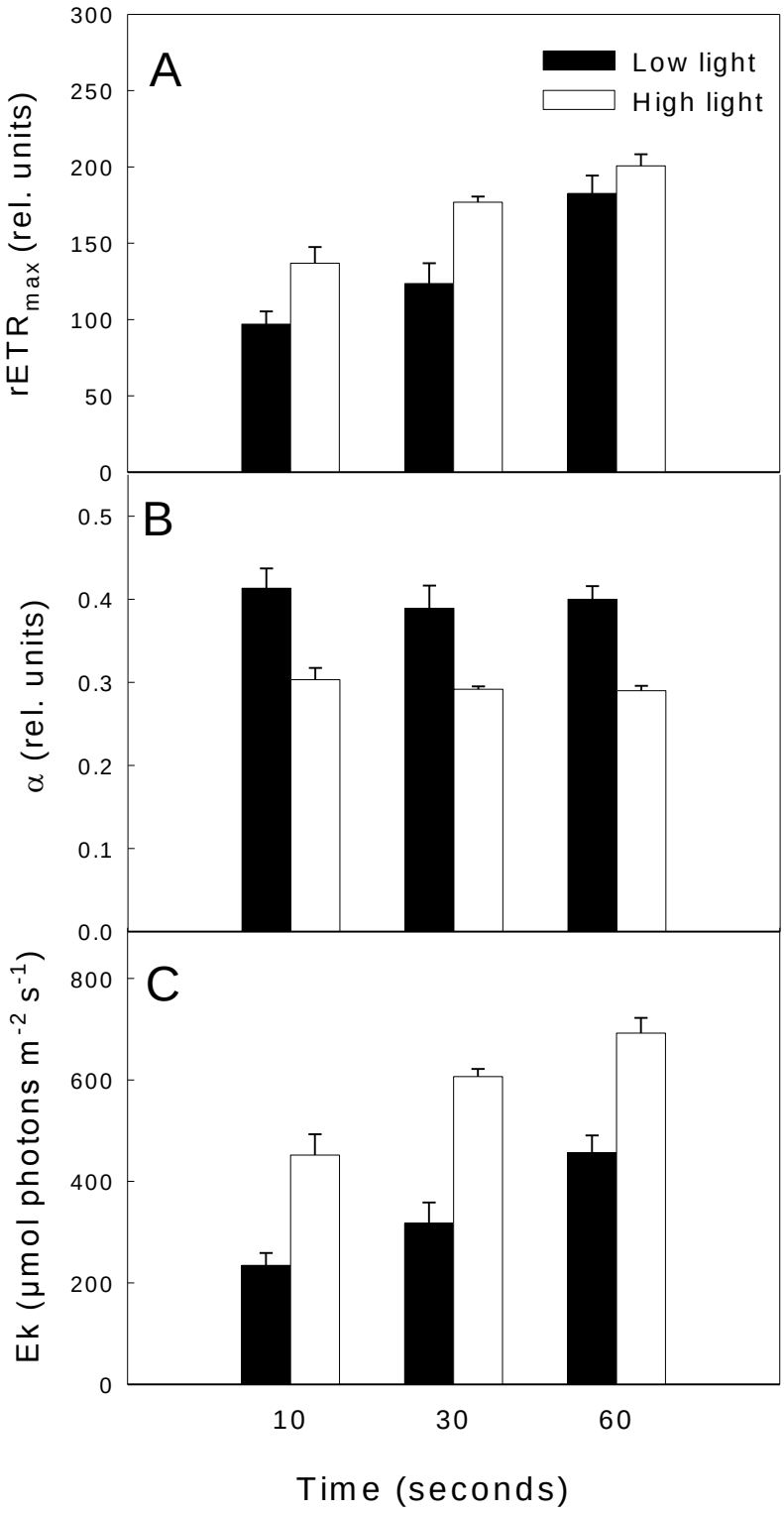

783

784

785 Figure 3

786

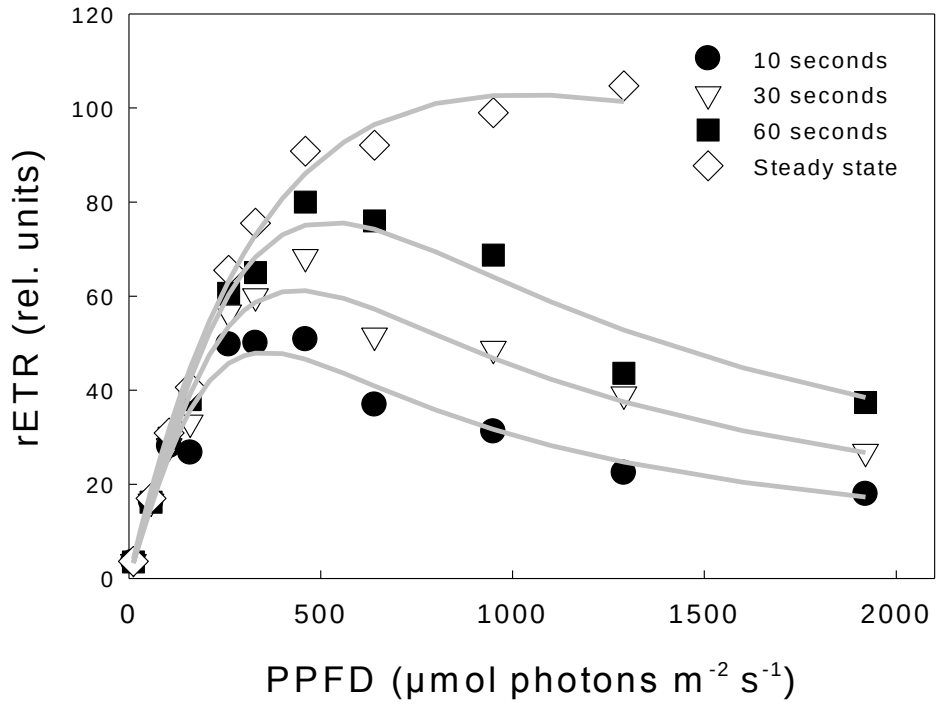

787

788

789

790

Figure 4

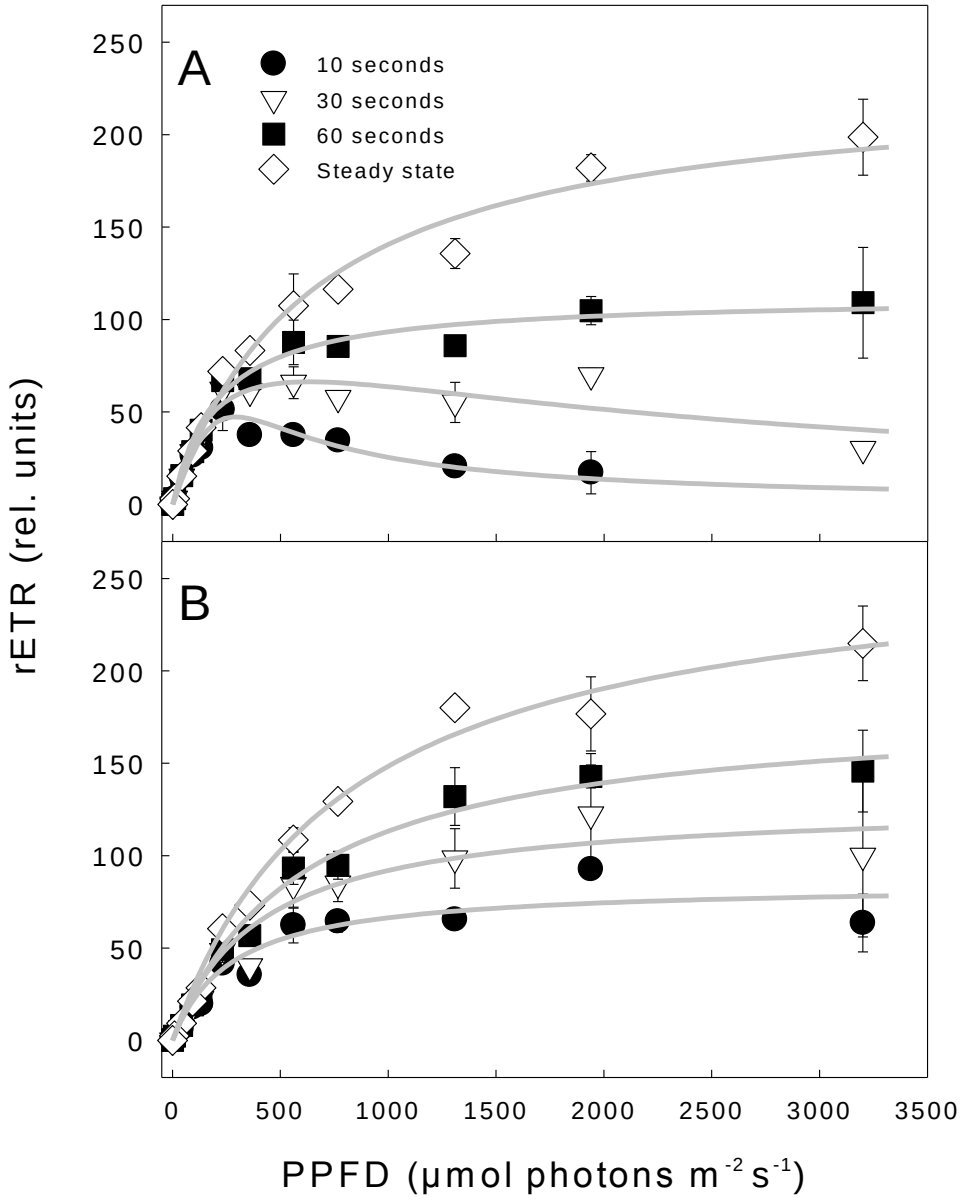

791

792

793

794

795

Figure 5

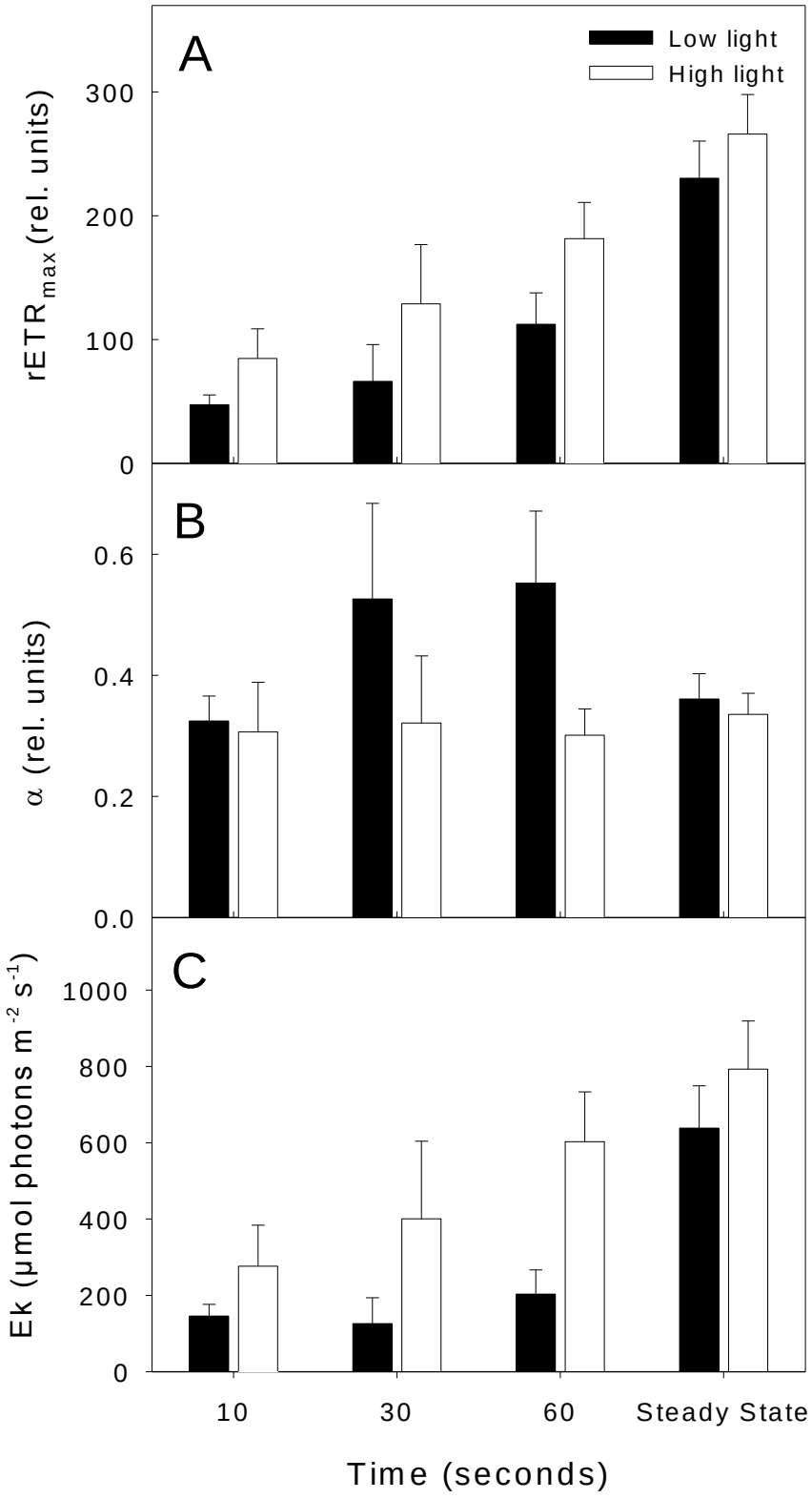

796

Figure 6

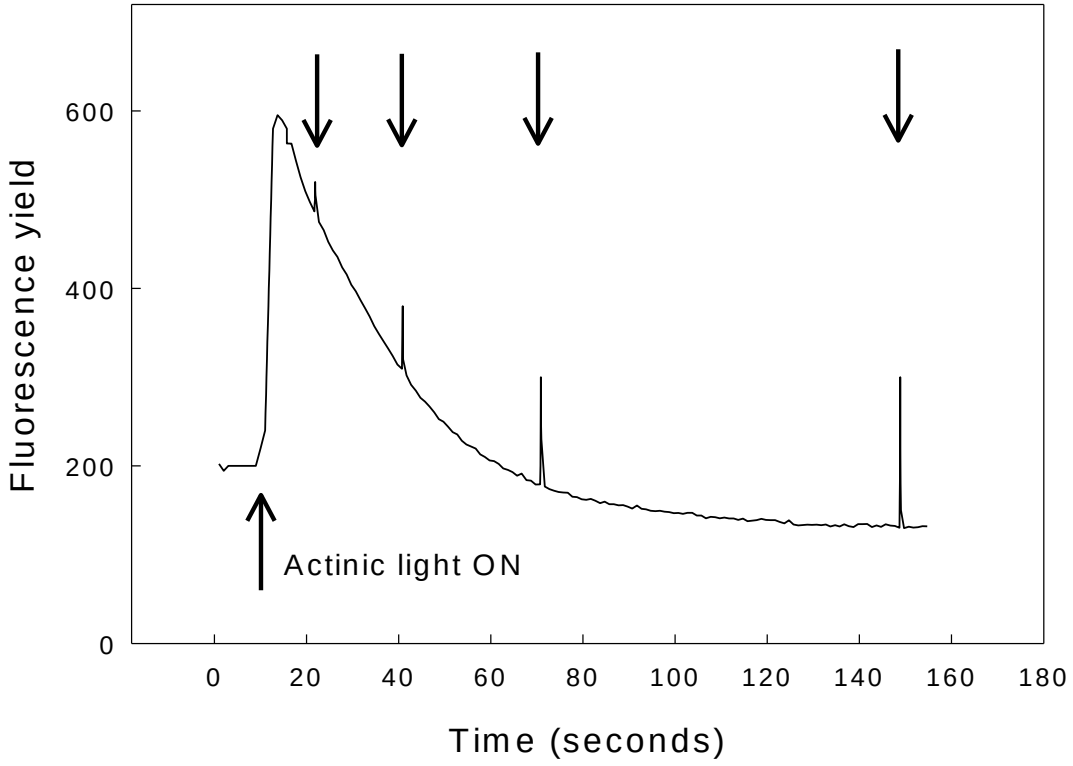
Fluorescence yield
600
400
200
0
0
20
40
60
80
100
120
140
160
180
Time (seconds)
Actinic light ON

805

Figure 7

806

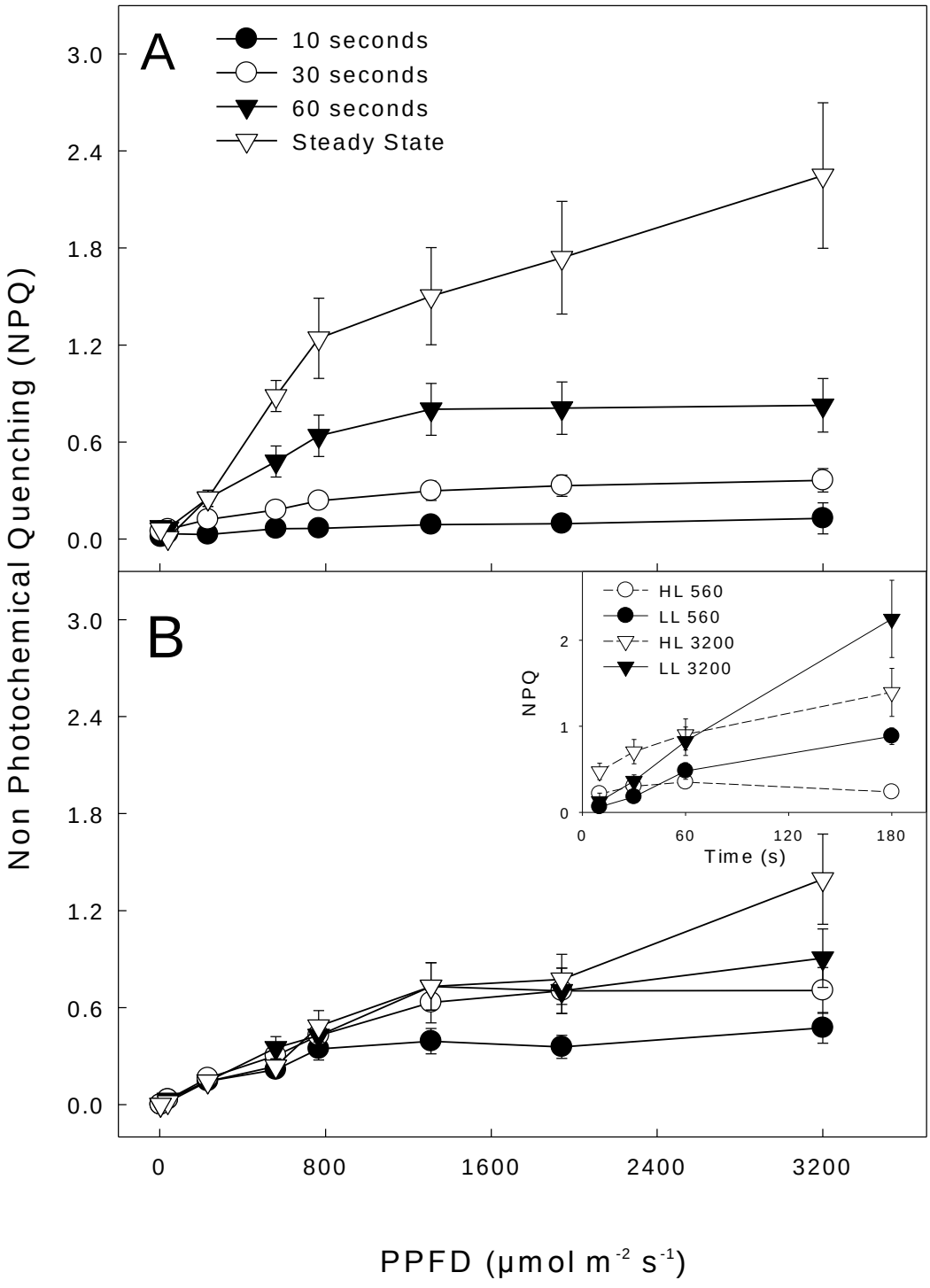

807

808